






Article

Multiple Geophysical Techniques for Investigation and Monitoring of Sobradinho Landslide, Brazil

Yawar Hussain ^{1,2,*}, Martin Cardenas-Soto ³, Salvatore Martino ⁴, Cesar Moreira ⁵,
Welitom Borges ⁶, Omar Hamza ⁷, Renato Prado ⁸, Rogerio Uagoda ⁹,
Juan Rodríguez-Rebolledo ¹, Rafeal Silva ¹ and Hernan Martinez-Carvajal ¹⁰

¹ Department of Civil and Environmental Engineering, University of Brasilia, Brasilia 70910-900, Brazil; jrodriguezr72@unb.br (J.R.-R.); rafael.silva@unb.br (R.S.)

² Environmental Engineering and Earth Sciences, Clemson University, Clemson, SC 29634, USA

³ Engineering Faculty, National Autonomous University of Mexico, Mexico City 04510, Mexico; martinc@unam.mx

⁴ Department of Earth Sciences and Research Center for Geological Risks (CERI), University of Rome “Sapienza”, 00185 Roma, Italy; salvatore.martino@uniroma1.it

⁵ Institute of Geoscience and Exact Science, São Paulo State University (UNESP), Sao Paulo 13506-900, Brazil; cesar.a.moreira@unesp.br

⁶ Institute of Geosciences, University of Brasilia, Brasilia 70910-900, Brazil; welitom@unb.br

⁷ College of Engineering and Technology, University of Derby, Derby DE223AW, UK; o.hamza@derby.ac.uk

⁸ Institute of Astronomy, Geophysics and Atmospheric Sciences, São Paulo University (USP), Sao Paulo 05508-090, Brazil; renato.prado@iag.usp.br

⁹ Department of Geography, University of Brasilia, Brasilia 70910-900, Brazil; rogeriouagoda@unb.br

¹⁰ Faculty of Mines, National University of Colombia at Medellin, Medellin, Colombia; hemartinezca@unal.edu.co

* Correspondence: yawar.pgn@gmail.com

Received: 30 September 2019; Accepted: 16 November 2019; Published: 26 November 2019



Abstract: Geophysical methods have a varying degree of potential for detailed characterization of landslides and their dynamics. In this study, the application of four well-established seismic-based geophysical techniques, namely Ambient Noise Interferometry (ANI), Horizontal to Vertical Spectral Ratio (HVSr), Multi-Channel Analysis of Surface Waves (MASW) and Nanoseismic Monitoring (NM), were considered to examine their suitability for landslide characterization and monitoring the effect of seasonal variation on slope mass. Furthermore, other methods such as Ground Penetrating Radar (GPR) and DC Resistivity through Electrical Resistivity Tomography (ERT) were also used for comparison purpose. The advantages and limitations of these multiple techniques were exemplified by a case study conducted on Sobradinho landslide in Brazil. The study revealed that the geophysical characterization of the landslide using traditional techniques (i.e., GPR, ERT and MASW) were successful in (i) the differentiation between landslide debris and other Quaternary deposits, and (ii) the delineation of the landslide sliding surface. However, the innovative seismic based techniques, particularly ambient noise based (HVSr and ANI) and emitted seismic based (NM), were not very effective for the dynamic monitoring of landslide, which might be attributed to the short-time duration of the data acquisition campaigns. The HVSr was also unsuccessful in landslide site characterization i.e., identification of geometry and sliding surface. In particular, there was no clear evidence of the light seasonal variations, which could have been potentially detected from the physical parameters during the (short-time) ambient noise and microseismic acquisition campaigns. Nevertheless, the experienced integration of these geophysical techniques may provide a promising tool for future applications.

Keywords: landslide dynamic; geophysical investigation; slope mass

1. Introduction

Landslides are one of the most hazardous natural phenomena [1], which have been investigated by a wide range of methods to define the geometry of landslides and collect information on stability conditions and state of activity [2]. These methods can generally be classified into two categories: intrusive, which may involve boreholes, soil sampling and laboratory testing, and non-intrusive, namely geophysical methods. The deployment of the latter has been increased exponentially for the subsurface characterization, localization of sliding surface, evaluation of the emergence and growths of fractures as well as for the understanding of water dynamics and possible reactivation by rainfall [3]. The information obtained from geophysical surveys is used as an input for defining ground models of landslides and consequently to perform slope stability assessment [4].

Geophysical investigations are principally applied at ground surface to measure the subsurface physical properties (e.g., seismic, gravitational, magnetic, and electrical) as well as anomalies in those properties. The techniques can support the determination of time-invariant (i.e., geometry, sliding surface location) and time-changing (i.e., saturation, mechanical properties and rheology) features [5,6]. However, due to the complexity and variation of ground conditions as well as the experimental site constraints, the efficiency of the geophysical methods may significantly vary. Therefore, further research concerning the suitability of these methods is highly required to examine, enhance and improve their applications.

This paper aims at examining the suitability of multiple advanced seismic-based geophysical techniques for the monitoring of seasonal variation and site characterization of landslide slopes. These were exemplified by a case study conducted on Sobradinho landslide in Ribeirão Contagem fluvial valley, Brazil. The case study represents a prototype of shallow and rainfall-triggered landslide i.e., commonly occurring phenomena in the region [7]. The dynamic analysis included three different advanced seismic geophysical techniques based on ambient noise including Ambient Noise Interferometry (ANI), Horizontal to Vertical Spectral Ratio (HVSr), and Nanoseismic Monitoring (NM). The investigation also used an emitted seismic (NM) as well as traditional seismic (Multi-Channel Analysis of Surface Waves-MASW) and non-seismic techniques such as Ground Penetration Radar (GPR) and DC Resistivity through Electrical Resistivity Tomography (ERT). The paper discusses the advantages and limitations of these techniques and reports some insight into their controlling factors. The study provides a rational basis for future research implementing geophysical methods for improving landslide investigation and stability assessment.

Background about the Seismic Techniques Used for the Landslide Investigation

Seismic techniques applied for studying landslide dynamics can be classified into two categories (i) ambient noise based (ANb) methods and (ii) emitted signal based methods (ESb). The ANb methods target the changes in wave-field properties generated by the variations in landslide mass properties occurring over time in response to active processes. While in ESb methods, seismic signals emitted by landslide movements (i.e., debris rearrangement, microfracturing or joint slipping) are captured and analyzed. Other techniques, which may be classified as traditional geophysical techniques, are also used for landslide site characterization that includes delineation of the slip surface, groundwater conditions, identification of permeable paths and litho-stratigraphy of the site.

Nano-seismic monitoring (NM), which is based on emitted signal (ESb), has been used for the dynamic analysis of landslides [8,9] as well as characterizing their activity [10]. Using NM, the effects of rainfall-induced pore-pressure and water conditions (stiffness variations) on the dynamics of landslides have been discussed in the literature [7,11,12]. The landslide dynamics are studied in terms of detection, characterization and localization of weak energy signals, named “slidequakes” (earthquake type having short-duration and are found discernable, traceable wave packets). Such signals are released because of rainfall-induced brittle failure in the landslide mass as reported in several previous studies e.g., [11–18]. Detailed typological review of these slidequakes is provided by Hussain et al. [9].

The slidequakes emitted from a deforming landslide mass are of low to very low magnitude and the heterogeneous soil conditions, a variable degree of saturation, and surface deformation quickly attenuates them [12]. Another difficulty that hinders their analysis is the uncertainty in the picking of P and S-waves arrivals based on traditional seismology. However, the associated microseismic emissions from landslides are confusing because of the involvement of two sources: (i) Endogenic-from deep within the landslide due to material deformation, and (ii) exogenic-from surficial processing such as rockfall and movement of debris and fluvial dynamics of the nearby rivers [12]. The separation of these two source mechanisms is of prime importance in any microseismic based landslide hazard assessment studies. In these cases, a simple and straightforward waveform and spectral analysis of the nano-signals become an attractive choice [12]. The emissions of microseismic signals for earthslides are still questionable. In the case of a clayey landslide, brittle materials are absent so energy is not suddenly released in the event of a collapse. However, sometimes the signals recorded are related to the mechanical behavior of soil [7]. Therefore, these techniques (SEb) are better described in comparison to some ground truth data provided by other complementary techniques such as remote sensing of the landslide surface and extensometer data that can significantly increase their reliabilities.

Under these conditions, ANb techniques such as time-lapse Ambient Noise Interferometry (ANI) and Horizontal to Vertical Spectral Ratio (HVSr) are preferred for landslide dynamic analysis, where the changes in landslide mass are inferred from the changes in the properties of ambient noise wave-fields recorded at different time. ANb is advantageous because: (i) Seismometers/geophones can be deployed inside as well as outside the landslide borders, (ii) it can be used as a continuous monitoring method because of the availability of ambient noise sources, (iii) it is non-invasive and low-cost tool especially suited for urban areas, (iv) data can be transmitted in real-time and analyzed automatically by software routines providing information about the landslide behavior, (v) no active sources such as earthquakes and explosives are necessary. The ANb techniques make use of ambient noise, with the vibrations of the ground caused by sources other than earthquakes. Recently, some authors [5,6,19–21] have found ambient noise as a potential and persistent source of energy that can be used for the understanding of the earth dynamics. This development has strengthened the applications of ANb techniques for the monitoring of landslides.

The dynamics of landslides using ANb techniques are monitored in terms of relative time-lapse changes in surface wave velocities (dV/V) obtained from ANI and changes in the natural period from time-lapse HVSr curve. These changes (dV/V and natural period) are produced because of rainfall-induced changes in the landslide mass such as rheology/rigidity [5,6], natural period [22] and pore-pressure induced stresses [23]. An anomalous change in the shear wave velocity (related to landslide seasonal dynamics and detected by ANI) is reported before the occurrence of a landslide [5], and their correlation with changes in the rheology of material is verified under controlled laboratory scaled experiment [24]. The other applications of ANI are stress changes with magma migration in the case of active volcanoes [25–27], structural images i.e., in the case of oil and gas [28], stress changes due to active faults [29,30], stress level monitoring in gold and silver mining [31], deep earth investigation [32,33], monitoring of civil and geotechnical structures like buildings [34–36], temporal changes in earthen embankments [19] and tailing dams [37].

Among the ANb techniques, HVSr, in particular, has many advantages because it offers a logistically efficient and cost-effective method to map landslide and its dynamics [38]. It provides information about the resonance behaviors of engineering-geological and geomorphological features. It has been applied extensively in landslide hazard assessment [21] and vulnerability to different triggering factors like earthquakes and rainfalls. However, in rainfall-induced saturation, it reduces impedance contrast by inducing changes in the rheology of the upper unconsolidated material, as is the case with a clayey landslide. It is the base for the application of HVSr for the analysis of seasonal dynamics of the rainfall-triggered landslide [39,40]. Other environmental studies where HVSr has been applied includes changes in ice thickness estimation [22,38,41] and its dynamics [42], estimation

of soil compaction [43] and for the monitoring of fluvial systems [44]. For landslide-affected areas, HVSR can show the directional effect as demonstrated in several studies [39,45–50].

The second step of composite landslide investigation is the site characterization that includes delineation of geometry, slip surface, permeable paths and evaluation of groundwater conditions. For geophysical site characterization, the traditional (ERT, GPR), as well as seismic based geophysical techniques (MASW and HVSR), are used. A detailed review of these techniques is available in the literature [3,51].

The severe drawbacks with respect to other in situ geotechnical techniques, geophysical based approaches are mainly due to the complexity of geology in landslide slopes. Nevertheless, these can be minimized by combining the geophysical results with the information obtained from engineering-geology and remote sensing data. Under non-ideal scenarios, the determination of impulse response by ANI method becomes challenging, especially if the target is noise-based tomography and less prominent in the case of monitoring [19]. Fractures at the surface attenuate the Rayleigh waves at short distances. In order to record these surface waves, a dense network of sensors is required, however this would increase the cost of the experiment due to their high spatial variability along the ground surface [52]. Therefore, the applications of ANI and other passive surface wave-based techniques at higher frequencies are not recommended in case of landslides. HVSR technique is based on 1D assumption, i.e., the material changes only with depth which is not the case with most landslides where lateral changes are also expected. Another difficulty with the HVSR is the presence of non-removable transient noise events that make results unreliable. The correct peak identification becomes a challenging task in the case of low subsurface impedance contrast [22] and the presence of two peaks on the HVSR curve.

From the above literature review, it can be concluded that geophysical methods have a significant potential for characterizing landslides and assessing the dynamic development of slope mass, but with varying success. Therefore, further research is required to evaluate their suitability in relation to the investigated landslide conditions.

2. Case Study of Sobradinho Landslide

2.1. Landslide Characterization

Ribeirão Contagem watershed is extended over 146 km² and located in the northern part of the Federal District of Brazil (Brasilia) in the Sobradinho administrative unit. The Maranhão River is the main tributary of the watershed that flows in the north and northeast directions. The drainage and channel densities of the watershed are 5.7 km/km² and 32.9 channels/km², respectively. The climate in the area is semi-humid tropical with a rainy summer and dry winter. The mean annual precipitation in the area is 1,442.5 mm and it is mainly related to rainfalls [53].

The selected slope is located in the Federal District of Brazil near a farm in a small vicinity named 'Rua do Mato' (Figure 1). The landslide is E-W trending rototranslational earthslide [54] and approximately 150 m long and 70 m wide. Along with the main scarp at the top of the landslide mass, there is a small scarp in the middle created by differential erosion produced by the release effects of the Contagem River, which is quite high during the rainy season. Sobradinho landslide is a typical Brazilian landslide (shallow and rainfall triggered).

The geology of Brasilia has been revised and updated in the form of the new geological map. Four lithological boundaries are distinguished: (i) Paranoá (metasedimentary rocks), (ii) Canastra (phyllites), (iii) Araxá (schists), (iv) Bambuí (clayed metasilites rolled, clay and metasilites banks) and (v) Groups and soil or shallow colluvial deposits (pedimentary type). These lithological units are present in reverse successions where the older unit lies above the younger ones. The geological setting of the succession mentioned above is mainly related to thrust faulting [55].

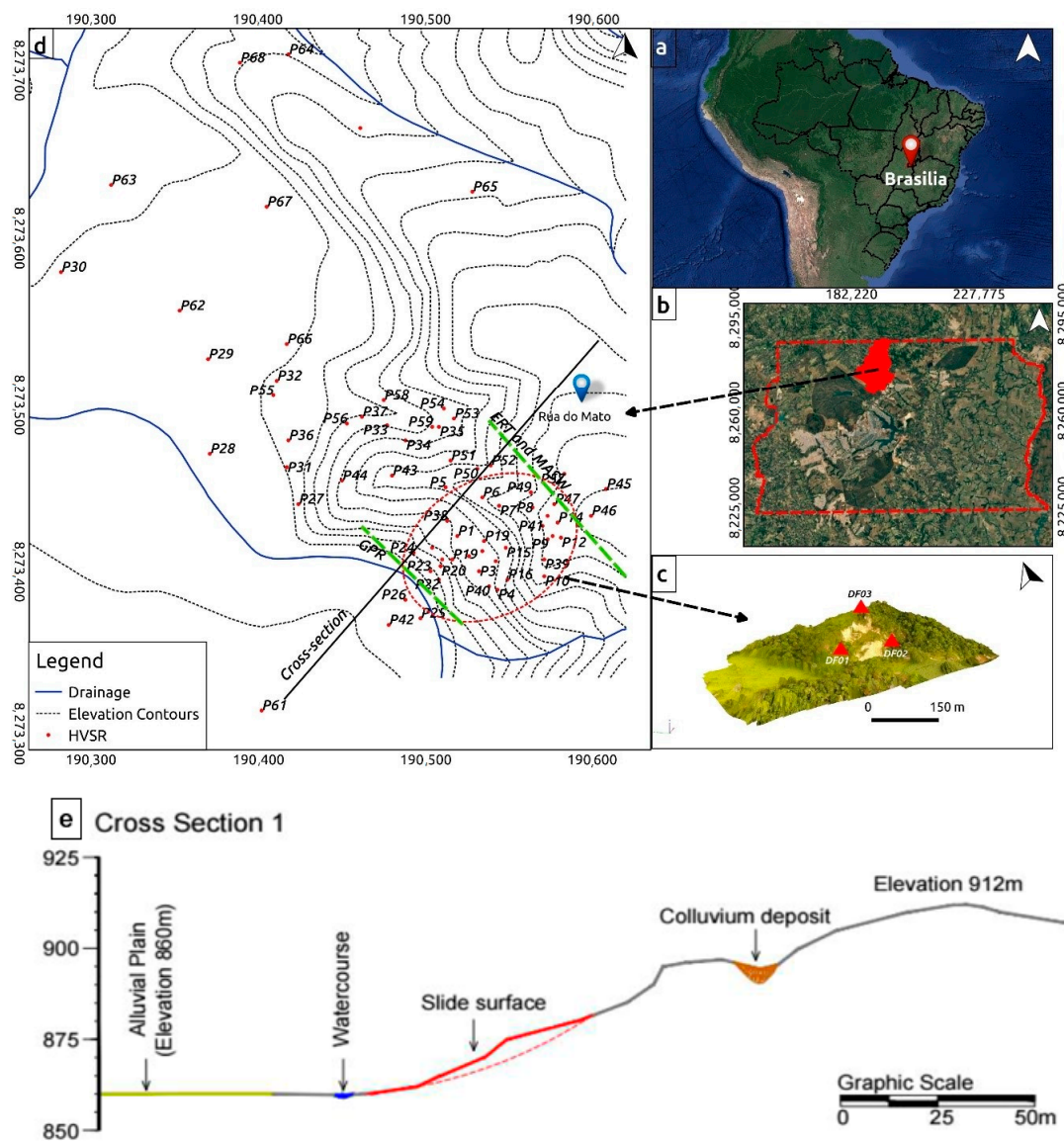


Figure 1. (a) Location of Brasília on the map of Brazil, (b) location of Ribeirão Contagem watershed on the map of Brasília, (c) Sobradinho landslide along with HVSr measuring points (red dots), ERT, MASW and GPR profiles locations (dotted green lines). The red dashed ellipse is the approximate landslide boundary and (d) zoomed drone landslide image with a triangular array used for time-lapse monitoring, (e) Along the black line, the cross-section of the landslide is drawn.

The region of Brasília is covered by a mantle of Tertiary-Quaternary age debris-lateritic soil composed mainly of red-yellow latosols. The thickness of soil cover is not constant and it varies from centimeters to tens of meters depending on the topography, vegetation and type of parent rocks. The soil in the region is named as ‘porous clays’ having high porosity and low density which is formed as a result of high degree of weathering and leaching. Due to its high porosity and cementitious bond type, it becomes a highly unstable under increased moisture and/or changes in the state of stresses, almost always presenting a volume variation as high as the variation of these factors (referred to as a collapsed structure) [7].

2.2. Materials and Methods

Methodologically, the study was carried out in two steps as site characterization and dynamic monitoring. In the site characterization, it is necessary to study the properties related to the dynamic

of landslide such as permeable paths, presences of fractures, landslide slip surface, landslide boundary and presence of a permeable layer at depth. The presence of the permeable layer at depth can cause a horizontal movement of infiltrating water which creates pore pressure in the landslide mass. It is a prevalent cause of reactivation of colluvial landslides in Brazil [23]. Therefore, the present study conducted a site investigation using a combination of geotechnical and geophysical techniques. The following methodological steps were carried out.

- The analysis of landslide slope began with the site characterization of a small geomorphological active basin, where the Contagem River flows and presents different geomorphological units such as alluvium, colluvial and sandy bars. The material characterization was carried out by conducting Particle Size Distribution (PSD) tests on the samples recovered from different locations in the areas in such a way that covers all the geomorphological units. Three topo-sequences were drawn for the investigation of the materials present in distinct morphologies slopes (closed concavity, open concavity and convex-rectilinear slope). Six undisturbed samples were collected for direct shear testing to determine the strength of materials i.e., cohesion and friction angle required to assess the stability condition and propensity of slope to collapse [56].
- After the in-situ soil testing [56], geophysical techniques (traditional as well as seismic based) were applied for the landslide site characterization. Each applied technique works on specific physical properties of the site such as electrical (ERT), electromagnetic (GPR) and elastic (seismic) [3]. The seismic based site characterization included the following tasks: delineation of the eroded boundary of the landslide, and the degree of compaction as a function of different depositional sequences, single station HVSR measurements, frequency-wavenumber (f-k) analysis and MASW were taken at the landslide mass and in the surrounding areas (Figure 1). Data for the HVSR were recorded with a three-component seismometer following [57] recommendations. HVSR curves were analyzed and the possible boundary of landslide was delineated based on the resonance frequency of the soil blocks. In the first stage, HVSR curves taken at different points both inside and outside the landslide were used for the determination of the possible extension of the unstable area. These curves were inverted together with dispersion curves (HVinv) obtained from the f-k analysis. These inversions resulted in shear wave velocity profiles of the landslide that are used for the determination of the landslide slip surface. The dispersion curve was obtained from the f-k analysis on the ambient noise records of a V-shape array of nine seismometers [58]. The MASW data were acquired along a profile selected in such orientations that covers the area of interest. The 48 channel Geode (Geometrics Inc.) seismograph along with 14 Hz geophones were used for the data acquisition. The seismic source used was a hammer of 8 kg that struck against a metal plate placed on the ground. Energy generation at each point was repeated (5 and 15 times) and stacked in this way the signal to noise ratio was improved.
- The next acquisition was carried out for the site characterization (time-invariant) of the landslide site included traditional geophysical techniques ERT and GPR. The aim of the GPR and ERT survey is to map the slip surface of landslide (electromagnetic and electrical resistivity contrasts) and to identify the presence of fractures and any cracks filled with the coarse and unconsolidated material (that pose different resistivity values compared with the surrounding lithologies). In ERT, the electric resistivity data were collected using a single channel acquisition system of 36 electrode Iris Syscal electric resistivity system with a 5 m electrode separation of the dipole-dipole array (Figure 2). The geophysical equipment of GPR consisted of a GSSI, Inc. SIR3000 GPR system, with a central frequency 400 MHz antenna, Syscal pro resistivity meter, 24 channels Geocode Seismograph with 14 Hz vertical component geophones. During the GPR data acquisition, precautions such as running the cart, its speed and sampling frequency were considered. Soil analysis was conducted using the samples recovered before the execution of the GPR profiles and also during the fieldwork, aiming at the comparison with GPR data. The material property contrast may help to understand different behaviors of the electromagnetic wave amplitude [59].

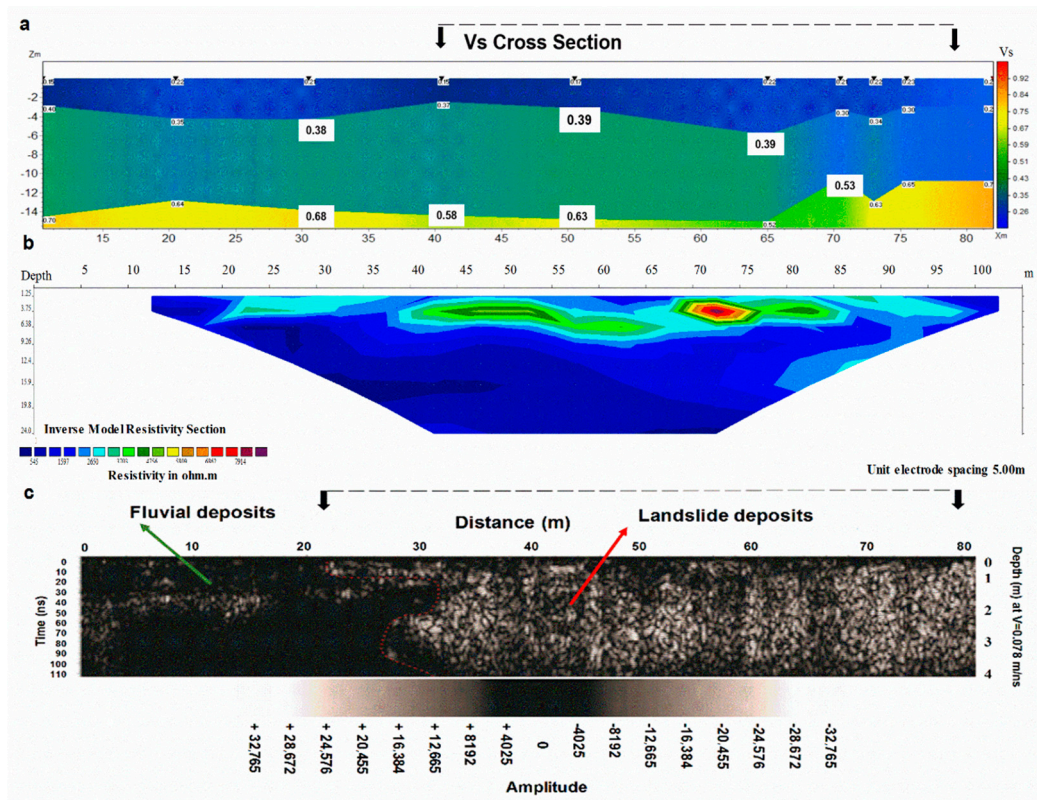


Figure 2. Results of (a) MASW and (b) ERT profiles that passes over landslide modeled electrical resistivity (Ohm.m) values and shear wave velocity (V_s) in km/sec, respectively. (c) GPR results taken at the base of landslide showing reflection amplitude. The interface between fluvial and landslide deposits is marked with dotted red lines [59]. The scales of these figures are different.

- After the site characterization, the analysis of seasonally changing landslide dynamics was carried out. For the dynamic analysis, two known ambient noise-based techniques i.e., Horizontal to Vertical Spectral Ratio (HVSr) and Ambient Noise Interferometry (ANI) were applied. The changes in ambient noise fields (HVSr and ANI) recorded at different times, helped infer the dynamic changes in the landslide mass while the microseismic emissions produced inside the landslide mass in response to rainfall-induced changes helped for the understanding of landslide dynamics itself. The continuous ambient noise recordings were done, at three fixed positions on the landslide in a triangular geometry, that covered mostly the landslide dynamically active regions with good azimuth coverage. The continuous data for the seasonal impact evaluation were recorded. The stations were named as DF01, DF02, DF03 (Figure 1). Time-lapse HVSr and ANI were applied at the same data.
- In the last section, microseismicity associated with soil failure and rainfall-induced stress-relief mechanisms were monitored. Nanoseismic Monitoring (NM) was applied, which is a highly specialized technique. Two mini-arrays of 20-m and 30-m apertures were developed during dry and rainy days. The microseismic records of landslide may possibly come from endogenic (related to dynamics of landslide itself) and exogenic (processes on the landslide like rock, debris flows and the nearby rivers etc.) source mechanisms. For the separation of endogenic from the exogenic processes, a typological analysis of the microseismic signals released in response to the degree of deformation in the soil of the study area is used. Same acquisition system was used as of ANI techniques. However, here seismometers were arranged in a mini-arrays of four sensors as explained by [7].

3. Results

3.1. Site Characterization

Three well-defined soil layers that provide different behaviors for each portion of the slope and valley bottom can be deduced from the geotechnical investigations. Higher shear strength values for all the portions of the slopes and the convex-rectilinear showed the highest value (68.11 kPa). The tests indicated a material with low cohesion and friction angle in the valley area. The failure envelope curves showed high shear stress supported by the convex slope soils at the expense of others. Detailed descriptions can be found in [56] and [59].

The results of MASW over specific profile showed fundamental and first higher mode dispersion curves [60]. However, only the fundamental mode of dispersion curve was used in the inversion process. The interpolation of the results of different 1D Vs profiles resulted in 2D plots showing the shear wave velocity variation (Figure 2b). The MASW profile showed larger fluctuations in S-wave velocity at the area directly above the landslide (Figure 2b) possibly related with the deformation of the subsurface associated with the onset of landslide event or because of the tomographic undulations of the deeper seismic bedrocks in the area. However, an increasing trend of S-wave velocity was observed indicating the increase in layer stiffness of the strata. The values of S-wave velocity are reasonably high indicating the stability of strata. However, there is a possibility of reactivation of the landslide at slip surface in extreme meteorological event because of pore water pressures and rheological changes in the landslide body combined with the river erosion at the bottom [7]. On the GPR profile (Figure 2c), the landslide material is well separated from the surrounding materials. These results were compared with soil sampling analysis [59].

The ERT profile covers the landslide body showing a continuous contrast that could be associated with the presence of a sliding surface (Figure 2). The small scale discontinuities of intermediate resistivity materials are also delineated on the section. The resistivity values suggest that they consist of relatively coarse-grained material, which may provide the pathways for the rainfall infiltrating water that may build pore water pressure in the landslide mass, that eventually, reactivating the landslide in the case of some future extreme rainfall events [7,23]. At the bottom, very low resistivity values were found that might be related to fine-grained material having a large amount of water (water table).

The ambient noise based HVSR curves showed the first peak at 2 Hz and a secondary peak at higher frequencies, ranging from 4 up to 6 Hz (Figures 3 and 4). The secondary peak may possibly be related with the frequency of the landslide mass, i.e., to the impedance contrast between landslide mass and its undeformed geological bedrock [38]. The measurements were carried out in two zones: Zone-A where ambient measurements were taken inside the landslide and Zone-B where ambient measurements were taken outside the apparent landslide boundary. The peak at 2 Hz is present everywhere in the area, while the secondary peak appears only within the landslide boundary. The ubiquitous peak may possibly be related to the bedrock in the area (Paranoá Group, carbonate rocks of Quaternary age). The depth of the bedrock is 27.5 m as calculated using the following formula $f_0 = V_s/4H$ [20] where 'fo' is the resonance frequency, 'H' is the depth and 'Vs' is the S-wave velocity. The adopted S-wave velocity was 220 m/sec, obtained from the MASW data.

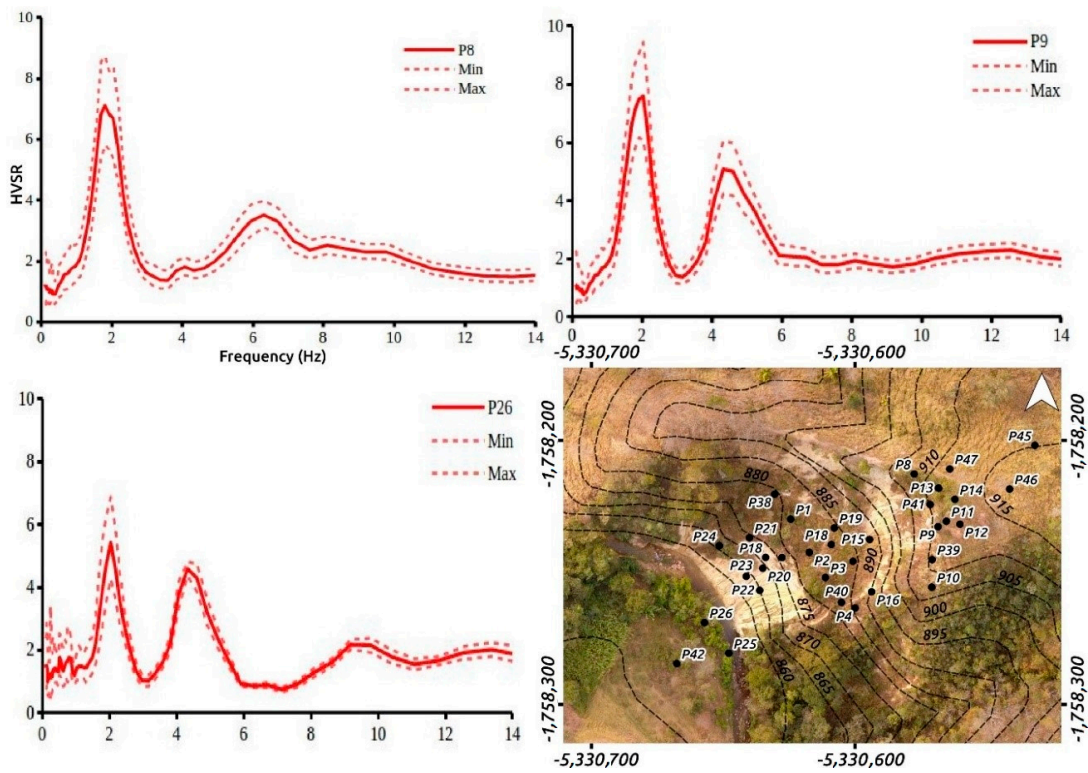


Figure 3. HVSR functions resulting in the measurement stations located inside the landslide mass. Solid and dotted lines are the average, minimum and maximal error values.

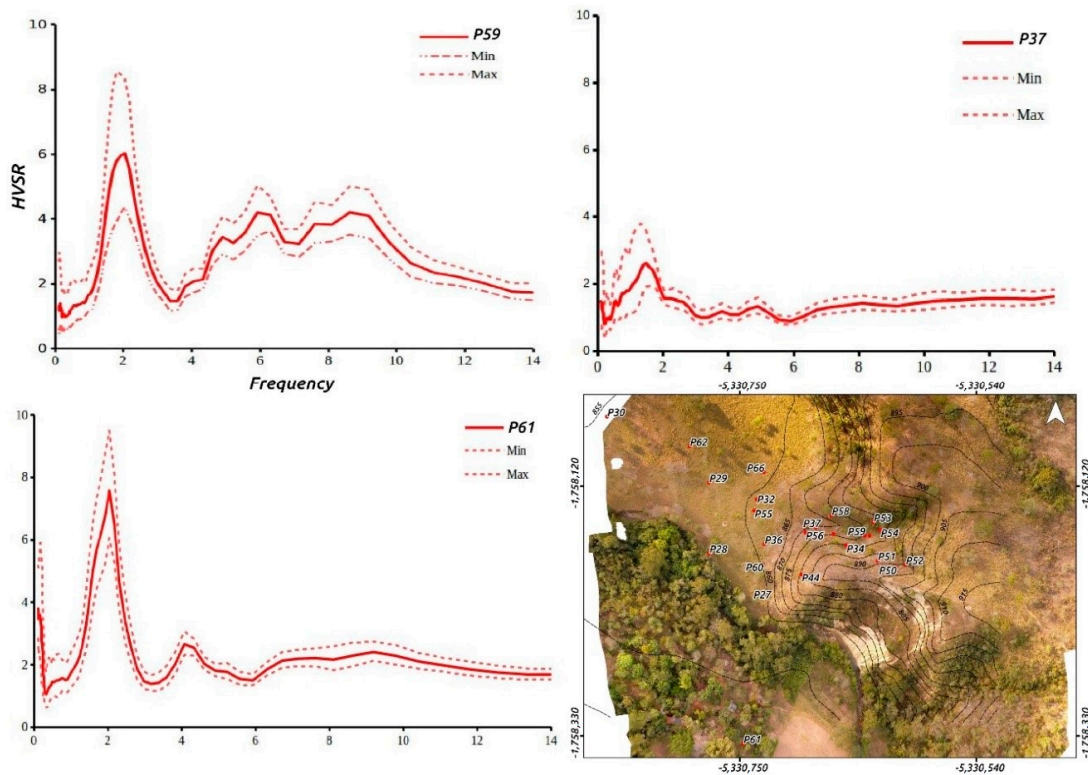


Figure 4. HVSR functions resulting in the measurements stations located outside the landslide mass. Solid and dotted lines are the average, minimum and maximal error values.

The landslide site characterization was also carried out by joint inversion of two curves (dispersion and HVSR). In this technique, HVSR and f-k dispersion curve were used. As a result, different sub-surface layers were delineated [58]. A velocity discontinuity at a depth of 7 m was assumed to be related with landslide slip surface (Figure 5). The overall velocity of the landslide site was found to be high which is consistent with the MASW results.

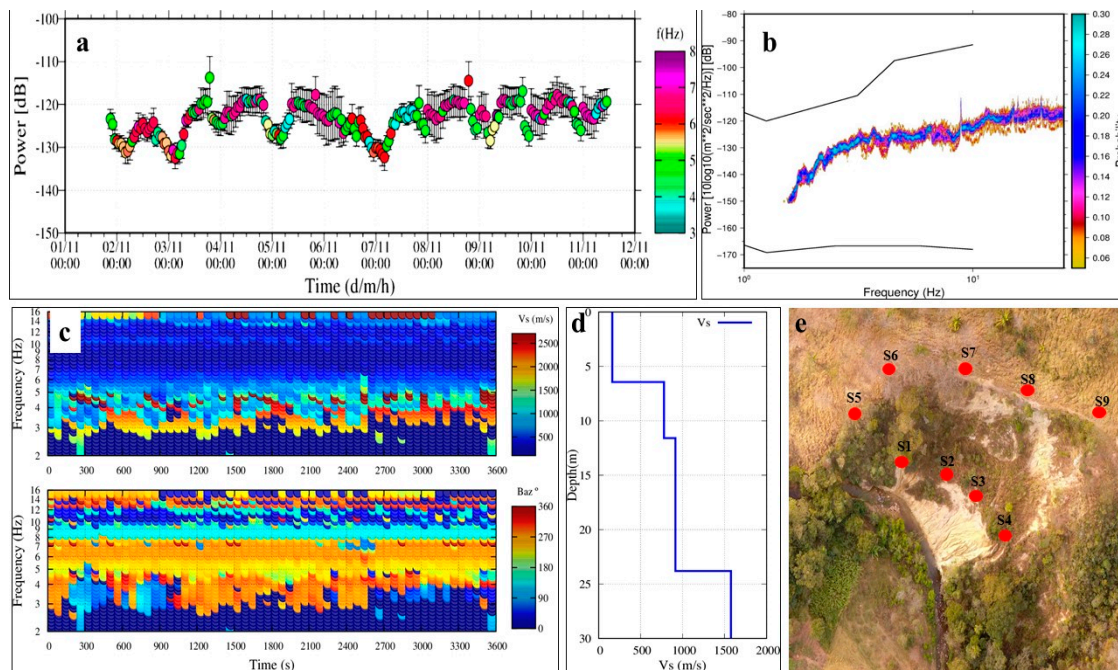


Figure 5. Results of initial ambient noise analysis in the area (a) Probability Density Function (PDF) of ambient noise record of station S1, (b) the mean value plus standard deviation colored with frequency values where mean values were calculated at S1 [61], (c) dispersion of recorded ambient noise wavefield S1, (d) Shear wave velocity profile of the site obtained after joint inversion of HVSR and dispersion curves [53], (e) V-shaped array of nine seismometers used for initial ambient noise analysis and shear wave velocity estimation.

ERT technique was able to mark the landslide slip surface while the presence of landslide on the MASW profile was not so clear, however, it showed some modification in VS values while passing over the landslide. These results are consistent with the inverted resistivity section obtained from MASW (Figure 2). The low signal to noise ratio of the MASW record made the interpretation dubious. Landslide slip surface was found at 8 m depth on resistivity profiles however, it was not possible to delineate the landslide slip surface using the MASW results (Figure 2). The result found by crossing Vs from MASW and HVSR by using the equation $f = Vs/4H$ it seems coherent that landslide mass.

3.2. Landslide Dynamics

The dynamic analysis of landslide using ambient noise starts with initial ambient noise analysis that includes calculation of ambient noise Power Spectral Density (PSD), Probability Density Function (PDF) and frequency wave-number analysis of the ambient noise recorded at the site. This analysis can provide information on the time-dependent variation in the ambient noise levels in the area as well as its frequency contents. In this preliminary analysis that frequency band is used which shows stability over time. The detailed methodology and the importance of ambient noise analysis are described in [53]. The results of ambient noise by spectral and f-k analysis shows that the ambient noise energy is stable in a frequency band 3–8; moreover, the ambient noise lies well between New High Noise Model (NHNM) and New Lower Noise Model (NLNM) (Figure 5).

In Figure 5c, average velocity values along 1 h time windows for each frequency are given. A large dispersion is observed before 5 Hz. Between 5 and 16 Hz the incoming wave field comes from 260 degrees but is not possible to obtain a dispersion curve. So the dispersion characteristics (phase velocity vs frequency) of surface become invisible after 6 Hz. Below 2 Hz there is no data of frequency response of the seismometers. The result indicates that incoming noise wave could compose of body waves at frequencies higher than 7 Hz.

After preliminary ambient noise analysis, the ANb geophysical techniques such as HVSR and ANI are applied on the ambient noise records from a triangular array of three seismometers. In Figure 6 the results of time-lapse monitoring using HVSR curve taken at rainy and non-rainy days are presented. It can be seen in Figure 6 that the stratigraphic peak at 2 Hz remained unaffected under different meteorological conditions (degree of saturation). Only HVSR peak amplitude variations are noticed; more in particular, these variations are not relevant for consistent stations S1, S3, S5, S6 while station S7 it shows a continuous decrease in peak amplitude during rainy days.

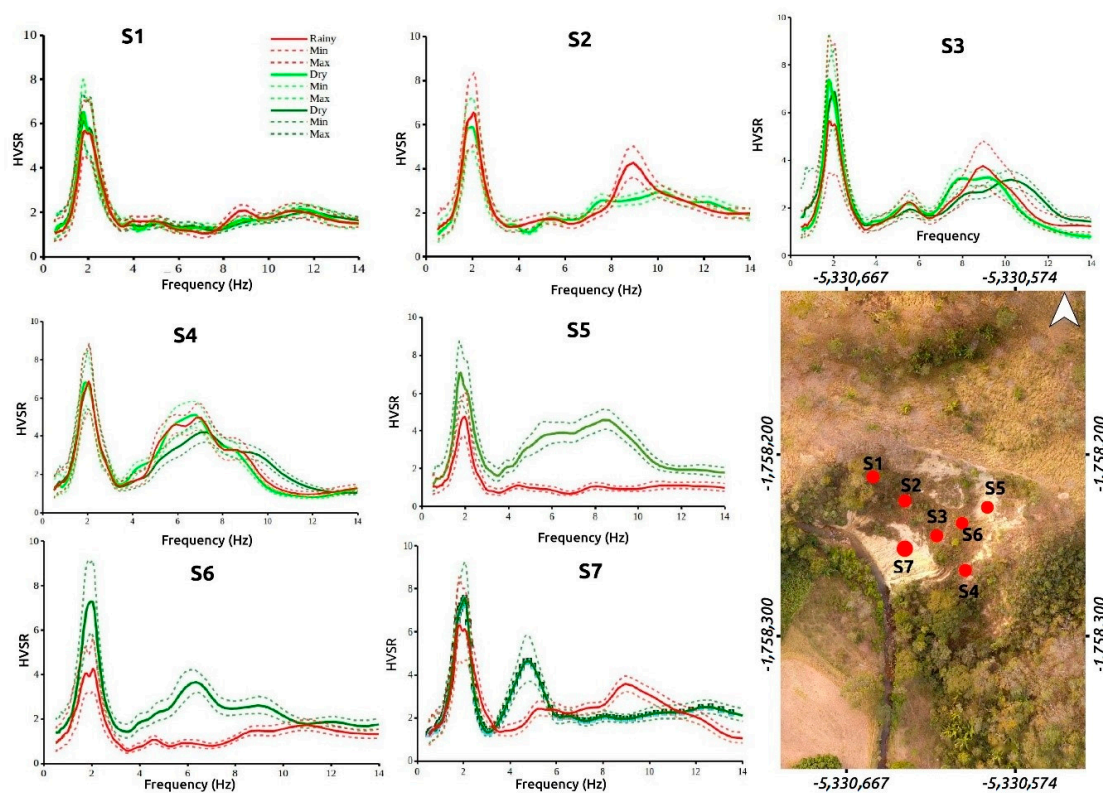


Figure 6. HVSR results of rainy hours (red) and non-rainy hours (light and dark green). The dotted lines express the standard deviation range while the solid line represents the average values. The insert in the figure shows the location of considered stations on landslide during rainy days.

On the contrary, it is interesting to note that there are other peaks at higher frequencies (4 up to 6 Hz) which appear and disappear during rainy and non-rainy days, respectively. These secondary peaks slightly appear during rainy days, however, their amplitude increased at stations S2 and S3 mainly because station S1 lies near the boundary of landslide as well as it was located at the elevated area, therefore, it did not get the predominant effects of rainfall. A new peak appears at stations S6 and S7 at frequency 6 Hz and 5 Hz, respectively during non-rainy days. This peak disappeared during rainy days (Figure 6). The peaks at station S5 during rainy days remained quite smooth while during non-rainy days because of ambient variations the secondary peaks disappeared. The seasonal dynamics inferred from time-lapse HVSR remained unambiguous. There is an absence of any unanimous feature on HVSR curves that can be linked with meteorological conditions and changes in the degree of landslide mass.

These results are consistent with the findings of preliminary ambient noise wavefield analysis which shows that the fluctuation in the ambient noise is stable in a frequency range of 3–8 Hz. It can be seen in Figure 7 that there are ambient noise peaks appear above 8 Hz. Unfortunately, the ANI results did not show any observable changes in the landslide dynamics in terms of calculated relative changes in the records ambient noise wavefield at different times (Figure 7). This may possibly happen because of the shorter duration of the ambient noise acquisition campaigns on landslides. A detailed discussion can be found at [62]. A similar phenomenon was observed by [63] at a clayey landslide where the results did not show any mark changes in dV/V . The sporadic variations which are evident in Figure 8 are possibly related to the changes in ambient noise wavefield.

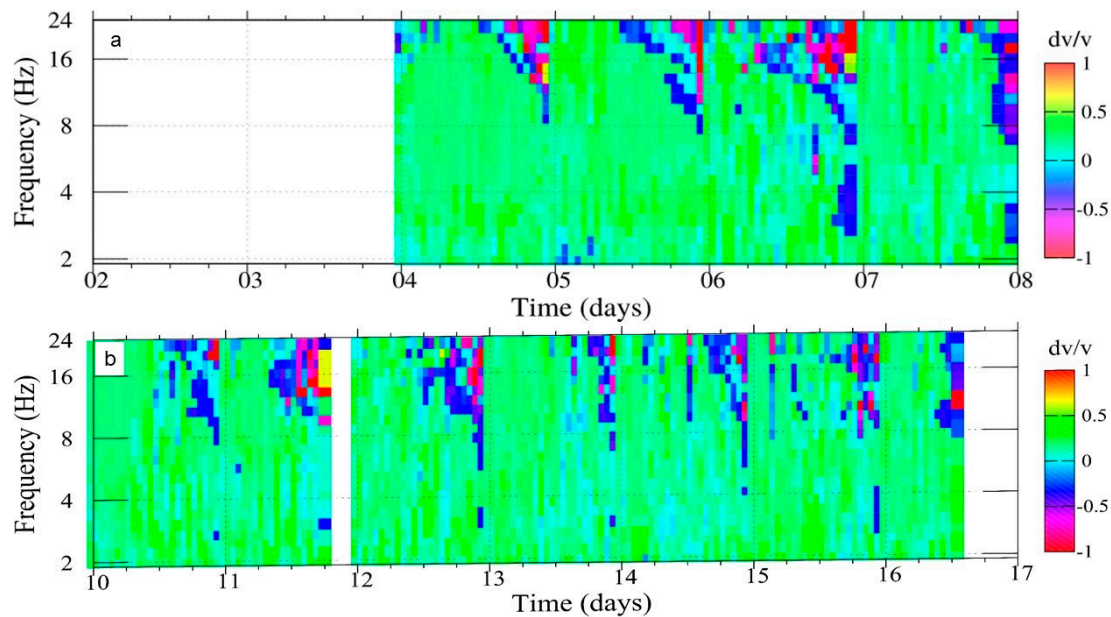


Figure 7. Time-lapse ANI results of ambient noise records of a triangular array of three sensors at landslide (a) dry and (b) rainy days. The color bars present values relative change in velocity (dV/V) [62].

The obtained results from time-lapse (4D) ambient noise records using non-standard seismological techniques ANI did not show any response to the rainfall-induced changes in the landslide mass. The ambient noise based HVSR technique showed some interesting results. The behavior of curves changes with the meteorological conditions. These changes were noticed at both primary and secondary peaks in terms of both peak frequencies and their amplitudes. Under shorter time window records it is difficult to assign these peaks with the degree of saturation.

The landslide dynamic analysis was also carried out based on the typological analysis of the nano-signals recorded at the mini-arrays of four sensors [7]. No distinct phase onsets could be identified on the records of the experiments that had made the event localization difficult, thus the event screening was done with the sonogram. The screening of the seismic record carried out with NanoseismicSuite [8], specially designed software for the characterization and localization of the weak energy events. Since different typologies of signals are observed during rainy seasons (Figure 8). Topology 11 is the noise in the record. The spiky signals were found and were presented as typology 4, 6 and 7 in Figure 8. Typologies 3, 9 and 10 are propagating in nature and might be related to river bedload [7].

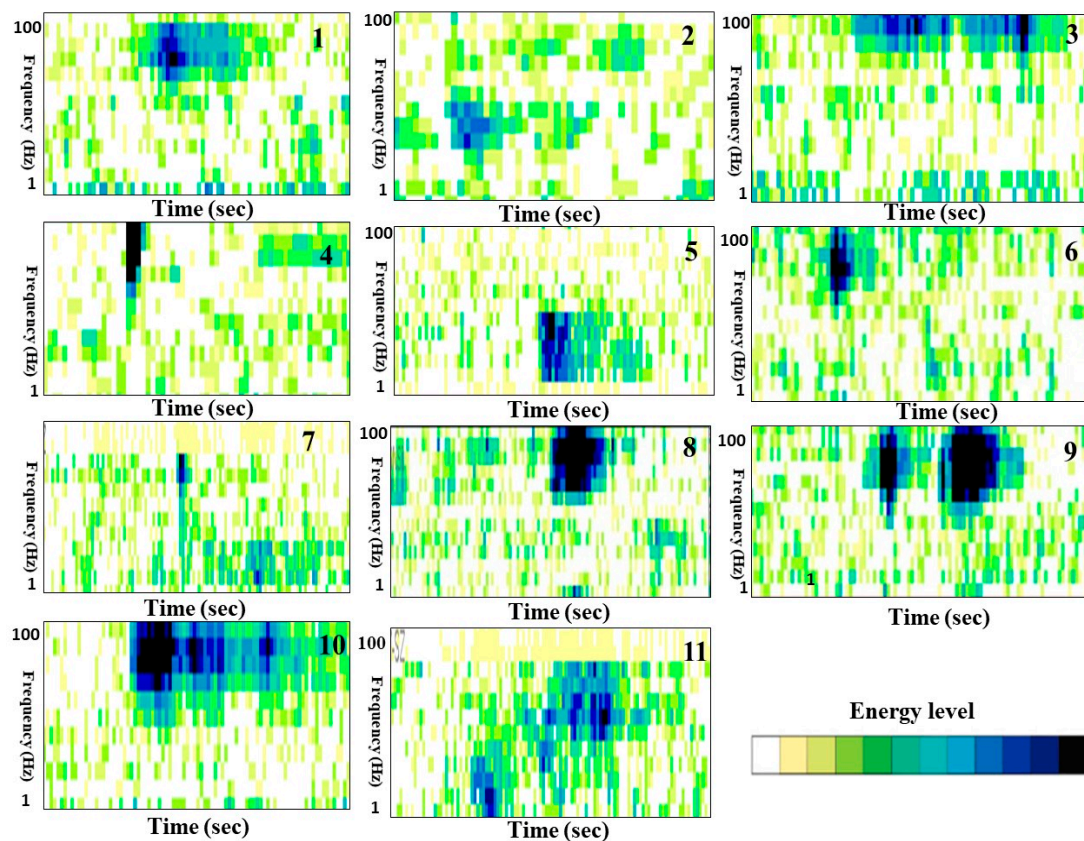


Figure 8. Typologies of supersonograms for microseismic signals recorded during the rainy days (from 1 to 11) at Sobradinho landslide only vertical component are considered [7].

4. Discussion and Conclusions

The geophysical techniques applied in this study (i.e., traditional and innovative) had initially two targets: (i) Site characterization and (ii) monitoring landslide dynamics. The site characterization using the three traditional methods (GPR, ERT and MASW) were successful in the differentiation of landslide debris and other Quaternary deposits as well as in detecting the landslide slip surface. However, the seismic (ambient noise) based technique (HVSr) reasonably helped in the landslide site characterization, i.e., outline the landslide boundaries (only 2nd peak within landslide) [64] and assess the thickness of the landslide mass based on a 1D resonance model [65].

The landslide site characterization was better carried out using standard geophysical techniques such as ERT and GPR. However, ANb technique such as HVSr remained ambiguous in achieving these objectives. On the other side, the non-standard seismological techniques were not so efficient in pointing out landslide dynamics. Too much disturbance in the site that leads to attenuation of seismic wave and the level of ambient noise in the zones close to landslide slope especially in urban areas. The non-standard seismic techniques were very effective in explaining the dynamics of landslide that might be related to the activation and reactivation of already existent slip surfaces. However, two issues were experienced: the short-term data acquisitions and the lack of full-saturation of landslide mass due to the shorter amount infiltration of rainfall during the data acquisition window. Another issue that hindered the performance of these techniques might be the significantly slow or lack of movement in the investigation area of the landslide. The ambient noise recorded at different level of soil saturation conditions were compared. The high porosity of the clayey deposits composing the landslide mass above 55% requires a large amount of water to reach its saturation point [63]. However, the recorded rainfall amount during the campaigns was small as a result the soil could not be saturated during the experimental fieldwork.

Regarding the site characterization, the following conclusions can be drawn: (i) There were small discontinuities filled with high resistivity materials over the horizontal and transverse directions of the landslide mass, which might be linked with saturation increment due to water infiltration after rainfall events. These could represent a source of pore water pressure elevation leading to landslide reactivation along pre-existing sliding surface in the event of extreme rainfall; (ii) the peak of 2 Hz (found in the entire area) might represent the site response of seismically low-velocity soft deposits ascribable to the Paranoá geological group overlying local seismic bedrock.

On the contrary, the advanced seismic based approaches were not adequately efficient in monitoring the landslide dynamics as explained by the following remarks: (i) No changes were visible within the local seismic record in response to the rainy and non-rainy months; (ii) the recorded microseismicity was most likely due to transportation of deposits by water i.e., not to landslide dynamics; (iii) no changes in the mechanical properties were detected over the investigation time. The results showed some signals that might be linked with the dynamics of the Contagem River. As there are changes in the flood level and bed-loading capacity of the river so these signals might be produced by the actions of sediments. During rainfall, the sediment carrying the energy of the river is expected to increase generating high seismic energies that might be detected by the nearby seismometer. Therefore, these signals are likely to have been generated by the river dynamic processes and not by the activities in the landslide itself. These exogenic mechanism (river generated seismicity) have also been reported in previous studies [7,12].

The integration of geophysical approaches, experienced in this study, provides a promising perspective despite the lack of evidence of the expected changes and variations of properties due to seasonal effects on the soil mass of Sobradinho landslide. The lack of dynamic evidence is probably associated with the following shortcomings: (i) Significant ambient disturbances because of the short time records, (ii) not representative meteorological conditions in the considered time-period, and (iii) insignificant time-changing landslide dynamic. For future studies, longer-term acquisition of the field data is highly recommended in order to overcome the issue of soil saturation and ambient noise disturbances.

The limitations of passive seismic monitoring such as high spatial uncertainty of the detected seismic events and hence speculative sources characterization can be improved by the involvement of remote sensing and geodetic datasets validated by the engineering-geological information of the area. Geodetic dataset can help in identifying exogenic effects from endogenic by comparing the microseismic events recorded by SNS with the geodetic results in order to check the possibility of any activity in the landslide slope (bulging or subsidence) or to rock walls (block falls or new fracturing) at the time of microseismic event record.

Author Contributions: Conceptualization, Y.H. and S.M.; methodology, Y.H.; software, Y.H., M.C.-S. and W.B.; validation, Y.H.; formal analysis, Y.H.; investigation, Y.H.; resources, Y.H.; data curation, Y.H., M.C.-S.; writing—original draft preparation, Y.H.; writing—review and editing, S.M.; and O.H.; supervision, S.M. and H.M.-C.; project administration, H.M.-C.; funding acquisition, Y.H. and H.M.-C., R.U., R.P., C.M., R.S., J.R.-R.

Funding: This research was funded by Research of the Federal District Foundation (FAPDF), and The APC was funded by the Department of Geography, University of Brasilia.

Acknowledgments: The authors acknowledge the support of the following agencies: the National Council for Scientific and Technological Development (CNPq), the Support Research of the Federal District Foundation (FAPDF), the University of Brasilia and, the Pool of Brazilian Equipment (PegBr), Rio de Janeiro. This section is not mandatory, but can be added to the manuscript if the discussion is unusually long or complex.

Conflicts of Interest: The authors declare no conflict of interest.

References

- Petley, D. Global patterns of loss of life from landslides. *Geology* **2012**, *40*, 927–930. [[CrossRef](#)]
- Cruden, D.M.; Varnes, D.J. *Landslide Types and Processes*; USGS: Reston, VA, USA, 1996.
- Pazzi, V.; Morelli, S.; Fanti, R. A Review of the Advantages and Limitations of Geophysical Investigations in Landslide Studies. *Int. J. Geophys.* **2019**, *2019*, 2983087. [[CrossRef](#)]
- Whiteley, J.S.; Chambers, J.E.; Uhlemann, S.; Wilkinson, P.B.; Kendall, J.M. Geophysical monitoring of moisture-induced landslides: A review. *Rev. Geophys.* **2019**, *57*, 106–145. [[CrossRef](#)]
- Mainsant, G.; Larose, E.; Brönnimann, C.; Jongmans, D.; Michoud, C.; Jaboyedoff, M. Ambient seismic noise monitoring of a clay landslide: Toward failure prediction. *J. Geophys. Res.* **2012**, *117*. [[CrossRef](#)]
- Harba, P.; Pilecki, Z. Assessment of time–spatial changes of shear wave velocities of flysch formation prone to mass movements by seismic interferometry with the use of ambient noise. *Landslides* **2017**, *14*, 1225–1233. [[CrossRef](#)]
- Hussain, Y.; Hussain, S.M.; Cardenas-Soto, M.; Uagoda, R.; Martino, S.; Rodriguez-Rebolledo, J.; Hamza, O.; Martinez-Carvajal, H. Typological analysis of slidequakes emitted from landslides: Experiments on an expander body pile and Sobradinho landslide (Brasilia, Brazil). *REM Int. Eng. J.* **2019**, *72*, 453–460. [[CrossRef](#)]
- Joswig, M. Nanoseismic monitoring fills the gap between microseismic networks and passive seismic. Special topic, Leveraging Technology. *First Break* **2008**, *26*, 117–124.
- Hussain, Y.; Martinez-Carvajal, H.; Cardenas-Soto, M.; Martino, S. Introductory review of potential applications of nanoseismic monitoring in seismic energy characterization. *J. Eng. Res.* **2019**, *7*, 65–80.
- Fiorucci, M.; Iannucci, R.; Lenti, L.; Martino, S.; Paciello, A.; Prestininzi, A.; Rivellino, S. Nanoseismic monitoring of gravity-induced slope instabilities for the risk management of an aqueduct infrastructure in Central Apennines (Italy). *Nat. Hazards* **2017**, *86*, 1–18. [[CrossRef](#)]
- Walter, M.; Walser, M.; Joswig, M. Mapping rainfall-triggered slidequakes and seismic landslide-volume estimation at Heumoes slope. *Vadose Zone J.* **2011**, *10*, 487–495. [[CrossRef](#)]
- Vouillamoz, N.; Rothmund, S.; Joswig, M. Characterizing the complexity of microseismic signals at slow-moving clay-rich debris slides: The Super-Sauze (southeastern France) and Pechgraben (Upper Austria) case studies. *Earth Surf. Dyn.* **2018**, *6*, 525. [[CrossRef](#)]
- Walter, M.; Gomberg, J.; Schulz, W.; Bodin, P.; Joswig, M. Slidequake Generation versus Viscous Creep at Softrock-landslides: Synopsis of Three Different Scenarios at Slumgullion Landslide, Heumoes Slope, and Super-Sauze Mudslide Slidequake Generation vs. Viscous Creep at Softrock-landslides. *J. Environ. Eng. Geophys.* **2013**, *18*, 269–280. [[CrossRef](#)]
- Gomberg, J.; Schulz, W.; Bodin, P.; Kean, J. Seismic and geodetic signatures of fault slip at the Slumgullion Landslide Natural Laboratory. *J. Geophys. Res.* **2011**, *116*. [[CrossRef](#)]
- Tonnellier, A.; Helmstetter, A.; Malet, J.P.; Schmittbuhl, J.; Corsini, A.; Joswig, M. Seismic monitoring of soft-rock landslides: The Super-Sauze and Valoria case studies. *Geophys. J. Int.* **2013**, *193*, 1515–1536. [[CrossRef](#)]
- Provost, F.; Hibert, C.; Malet, J.P. Automatic classification of endogenous landslide seismicity using the Random Forest supervised classifier. *Geophys. Res. Lett.* **2017**, *44*, 113–120. [[CrossRef](#)]
- Got, J.L.; Mourot, P.; Grangeon, J. Pre-failure behaviour of an unstable limestone cliff from displacement and seismic data. *Nat. Hazards Earth Syst. Sci.* **2010**, *10*, 819–829. [[CrossRef](#)]
- Bottelin, P.; Baillet, L.; Larose, E.; Jongmans, D.; Hantz, D.; Brenguier, O.; Helmstetter, A. Monitoring rock reinforcement works with ambient vibrations: La Bourne case study (Vercors, France). *Eng. Geol.* **2017**, *226*, 136–145. [[CrossRef](#)]
- Planès, T.; Mooney, M.A.; Rittgers, J.B.R.; Parekh, M.L.; Behm, M.; Snieder, R. Time-lapse monitoring of internal erosion in earthen dams and levees using ambient seismic noise. *Geotechnique* **2016**, *66*, 301–312. [[CrossRef](#)]
- Ullah, I.; Prado, R.L. Soft sediment thickness and shear-wave velocity estimation from the H/V technique up to the bedrock at meteorite impact crater site, Sao Paulo city, Brazil. *Soil Dyn. Earthq. Eng.* **2017**, *94*, 215–222. [[CrossRef](#)]
- Hussain, Y.; Martinez-Carvajal, H.; Condori, C.; Uagoda, R.; Cárdenas-Soto, M.; Cavalcante, A.L.B.; Luciano Soares da Cunha, L.S.; Martino, S. Ambient Seismic Noise: A Continuous Source for the Dynamic Monitoring of Landslides. *Terrae Didat.* **2019**, *15*, 103–107.

22. Martino, S. Earthquake-induced reactivation of landslides: Recent advances and future perspectives. In *Earthquakes and Their Impact on Society*; D'Amico, S., Ed.; Springer: Cham, Switzerland, 2016; pp. 291–322, ISBN 978-3-319-21752-9.
23. Ehrlich, M.; da Costa, D.P.; Silva, R.C. Behavior of a colluvial slope located in Southeastern Brazil. *Landslides* **2018**, *15*, 1595–1613. [[CrossRef](#)]
24. Mainsant, G.; Jongmans, D.; Chambon, G.; Larose, E.; Baillet, L. Shear wave velocity as an indicator for rheological changes in clay materials: Lessons from laboratory experiments. *Geophys. Res. Lett.* **2012**, *14*, 1225–1233. [[CrossRef](#)]
25. Sens-Schönfelder, C.; Wegler, U. Passive image interferometry and seasonal variations of seismic velocities at Merapi volcano, Indonesia. *Geophys. Res. Lett.* **2006**, *33*, L21302. [[CrossRef](#)]
26. Obermann, A.; Planès, T.; Larose, E.; Campillo, M. Imaging pre-eruptive and co-eruptive structural and mechanical changes of a volcano with ambient seismic noise. *J. Geophys. Res.* **2013**, *118*, 6285–6294. [[CrossRef](#)]
27. Delgado, J.; Garrido, J.; Lenti, L.; Lopez-Casado, C.; Martino, S.; Sierra, F.J. Unconventional pseudostatic stability analysis of the Diezma landslide (Granada, Spain) based on a high-resolution engineering-geological model. *Eng. Geol.* **2015**, *184*, 81–95. [[CrossRef](#)]
28. Bakulin, A.; Mateeva, A.; Mehta, K.; Jorgensen, P.; Ferrandis, J.; Herhold, I.; Lopez, J. Virtual source applications to imaging and reservoir monitoring. *Lead. Edge* **2007**, *26*, 732–740. [[CrossRef](#)]
29. Wegler, U.; Sens-Schönfelder, C. Fault zone monitoring with passive image interferometry. *Geophys. J. Int.* **2007**, *168*, 1029–1033. [[CrossRef](#)]
30. Brenguier, F.; Shapiro, N.M.; Campillo, M.; Ferrazzini, V.; Duputel, Z.; Coutant, O.; Nercessian, A. Towards forecasting volcanic eruptions using seismic noise. *Nat Geosci.* **2008**, *1*, 126–130. [[CrossRef](#)]
31. Gret, A.; Snieder, R.; Özbay, U. Monitoring in situ stress changes in a mining environment with coda wave interferometry. *Geophys. J. Int.* **2006**, *167*, 586–598. [[CrossRef](#)]
32. Boué, P.; Poli, P.; Campillo, M.; Pedersen, H.; Briand, X.; Roux, P. Teleseismic correlations of ambient seismic noise for deep global imaging of the earth. *Geophys. J. Int.* **2013**, *194*, 844–848. [[CrossRef](#)]
33. Lin, F.C.; Tsai, V.C.; Schmandt, B.; Duputel, Z.; Zhan, Z. Extracting seismic core phases with array interferometry. *Geophys. Res. Lett.* **2013**, *40*, 1049–1053. [[CrossRef](#)]
34. Snieder, R.; Safak, E. Extracting the building response using seismic interferometry: Theory and application to the Millikan Library in Pasadena, California. *Bull. Seismol. Soc. Am.* **2006**, *96*, 586–598. [[CrossRef](#)]
35. Nakata, N.; Snieder, R.; Kuroda, S.; Ito, S.; Aizawa, T.; Kunimi, T. Monitoring a building using deconvolution interferometry. I: Earthquake-data analysis. *Bull. Seismol. Soc. Am.* **2013**, *103*, 1662–1678. [[CrossRef](#)]
36. Nakata, N.; Snieder, R. Monitoring a building using deconvolution interferometry. II: Ambient-vibration analysis. *Bull. Seismol. Soc. Am.* **2014**, *104*, 204–213. [[CrossRef](#)]
37. Olivier, G.; Brenguier, F.; de Wit, T.; Lynch, R. Monitoring the stability of tailings dam walls with ambient seismic noise. *Lead. Edge* **2017**, *36*, 350a1–350a6. [[CrossRef](#)]
38. D'Amico, S.; Francesco, P.; Salvatore, M.; Roberto, I.; Antonella, P.; Giuseppe, L.; Pauline, G.; Daniela, F. Ambient noise techniques to study near-surface in particular geological conditions: A brief review. In *Innovation in Near-Surface Geophysics*; Elsevier: Amsterdam, The Netherlands, 2019; pp. 419–460.
39. Imposa, S.; Grassi, S.; Fazio, F.; Rannisi, G.; Cino, P. Geophysical surveys to study a landslide body (north-eastern Sicily). *Nat. Hazards* **2017**, *86*, 327–343. [[CrossRef](#)]
40. Bertello, L.; Berti, M.; Castellaro, S.; Squarzon, G. Dynamics of an active earthflow inferred from surface wave monitoring. *J. Geophys. Res. Earth* **2018**, *123*, 1811–1834. [[CrossRef](#)]
41. Picotti, S.; Francese, R.; Giorgi, M.; Pettenati, F.; Carcione, J.M. Estimation of glacier thicknesses and basal properties using the horizontal-to-vertical component spectral ratio (HVSr) technique from passive seismic data. *J. Glaciol.* **2017**, *63*, 229–248. [[CrossRef](#)]
42. Köhler, A.; Nuth, C.; Schweitzer, J.; Weidle, C.; Gibbons, S.J. Regional passive seismic monitoring reveals dynamic glacier activity on Spitsbergen, Svalbard. *Polar Res.* **2015**, *34*, 26178. [[CrossRef](#)]
43. Harutoonian, P. *Geotechnical Characterisation of Compacted Ground by Passive Ambient Vibration Techniques*; School of Computing, Engineering and Mathematics University of Western Sydney: Sydney, Australia, 2012.
44. Anthony, R.E.; Aster, R.C.; Ryan, S.; Rathburn, S.; Baker, M.G. Measuring mountain river discharge using seismographs emplaced within the hyporheic zone. *J. Geophys. Res. Earth Surf.* **2018**, *123*, 210–228. [[CrossRef](#)]
45. Burjánek, J.; Gassner-Stamm, G.; Poggi, V.; Moore, J.R.; Fäh, D. Ambient vibration analysis of an unstable mountain slope. *Geophys. J. Int.* **2010**, *180*, 820–828. [[CrossRef](#)]

46. Del Gaudio, V.; Wasowski, J. Advances and problems in understanding the seismic response of potentially unstable slopes. *Eng. Geol.* **2011**, *122*, 73–83. [[CrossRef](#)]
47. Panzera, F.; D'Amico, S.; Lotteri, A.; Galea, P.; Lombardo, G. Seismic site response of unstable steep slope using noise measurements: The case study of Xemxija bay area, Malta. *Nat. Hazards Earth Syst. Sci.* **2012**, *12*, 3421. [[CrossRef](#)]
48. Galea, P.; D'Amico, S.; Farrugia, D. Dynamic characteristics of an active coastal spreading area using ambient noise measurements—Anchor Bay, Malta. *Geophys. J. Int.* **2014**, *199*, 1166–1175. [[CrossRef](#)]
49. Iannucci, R.; Martino, S.; Martorelli, F.; Falconi, L.; Verrubbi, V. (2017, May). Susceptibility to Sea Cliff Failures at Cala Rossa Bay in Favignana Island (Italy). In *Workshop on World Landslide Forum*; Mikoš, M., Casagli, N., Yin, Y., Eds.; Springer: Cham, Switzerland, 2017; pp. 537–546. [[CrossRef](#)]
50. Iannucci, R.; Martino, S.; Paciello, A.; D'Amico, S.; Galea, P. Engineering geological zonation of a complex landslide system through seismic ambient noise measurements at the Selmun Promontory (Malta). *Geophys. J. Int.* **2018**, *213*, 1146–1161. [[CrossRef](#)]
51. Malehmir, A.; Socco, L.V.; Bastani, M.; Krawczyk, C.M.; Pfaffhuber, A.A.; Miller, R.D.; Maurer, H.; Frauenfelder, R.; Suto, K.; Bazin, S.; et al. Near-Surface Geophysical Characterization of Areas Prone to Natural Hazards: A Review of the Current and Perspective on the Future. In *Advances in Geophysics*; Nielsen, L., Ed.; Elsevier: Amsterdam, The Netherlands, 2016; pp. 51–146, ISBN 9780128095331.
52. Meza-Fajardo, K.C.; Varone, C.; Lenti, L.; Martino, S.; Semblat, J.F. Surface wave quantification in a highly heterogeneous alluvial basin: Case study of the Fosso di Vallerano valley, Rome, Italy. *Soil Dyn. Earthq. Eng.* **2019**, *120*, 292–300. [[CrossRef](#)]
53. Hussain, Y.; Martinez-Carvajal, H.; Cárdenas-Soto, M.; Uagoda, R.; Martino, S.; Hussain, B.M. Microtremor Response of a Mass Movement in Federal District of Brazil. *Anu. Inst. Geociênc.* **2017**, *40*, 212–221.
54. Hungr, O.; Leroueil, S.; Picarelli, L. The Varnes classification of landslide types, an update. *Landslides* **2014**, *11*, 167–194. [[CrossRef](#)]
55. Freitas-Silva, F.H.; Campos, J.E. Geologia do Distrito Federal. In *Inventário Hidrogeológico e Dos Recursos Hídricos Superficiais Do Distrito Federal*; SEMATEC, IEMA, MMA-SRH: Brasília, Brazil, 1998. (In Portuguese)
56. Braga, L.M.; Caldeira, D.; da Silva Nunes, J.G.; Hussain, Y.; Carvajal, H.M.; Uagoda, R. Caracterização geomorfológica e dinâmica erosivo-deposicional de encostas no vale fluvial do Ribeirão Contagem-DF, Brasil (in Portuguese). *Anu. Inst. Geociênc.* **2018**, *41*, 51–65. (In Portuguese)
57. SESAME Guidelines for the Implementation of the H/V Spectral Ratio Technique on Ambient Vibrations. Measurements, Processing and Interpretation. SESAME European Research Project WP12—D23.12. 2004. Available online: http://sesame-fp5.obs.ujf-grenoble.fr/Papers/HV_User_Guidelines.pdf (accessed on 20 February 2019).
58. Hussain, Y.; Cardenas-Soto, M.; Uagoda, R.; Martino, S.; Sanchez, N.P.; Moreira, C.A.; Martinez-Carvajal, H. Shear Wave Velocity Estimation by a Joint Inversion of HVSR and f-k Curves under Diffuse Field Assumption: A Case Study of Sobradinho Landslide. *Anu. Inst. Geociênc.* **2019**, *42*, 742–775. [[CrossRef](#)]
59. Nunes, J.G.; Uagoda, R.; Caldeira, D.; Braga, L.M.; Hussain, Y.; Carvajal, H.M. Aplicação do GPR para análise e diferenciação entre materiais aluvionares e coluvionares, embasadas em observações diretas, no vale do Ribeirão Contagem-Distrito Federal (Brasil). *Rev. Bras. Geomorfol.* **2019**, *20*. (In Portuguese) [[CrossRef](#)]
60. Hussain, Y.; Augoda, R. Site Characterization of Hillslopes in Ribeirão Contagem Fluvial Valley (Brasilia, Brazil) Using Geophysical Methods. In *Symposium on the Application of Geophysics to Engineering and Environmental Problems 2019*; Society of Exploration Geophysicists and Environment and Engineering Geophysical Society: Portland, OR, USA, 2019; pp. 403–408.
61. Hussain, Y.; Cárdenas-Soto, M.; Martinez-Carajal, H.; Uagoda, R.; Soares, J.; Martino, S. Spectral Analysis of the Recorded Ambient Vibration at a Mass Movement in Brasilia. In *Symposium on the Application of Geophysics to Engineering and Environmental Problems 2017*; Society of Exploration Geophysicists and Environment and Engineering Geophysical Society: Denver, CO, USA, 2017; pp. 214–218.
62. Hussain, Y.; Cardenas-Soto, M.; Uagoda, R.; Martino, S.; Rodriguez-Rebolledo, J.; Hamza, O.; Martinez-Carvajal, H. Monitoring of Sobradinho landslide (Brasília, Brazil) and a prototype vertical slope by time-lapse interferometry. *Braz. J. Geol.* **2019**, *49*, e20180085. [[CrossRef](#)]
63. Bièvre, G.; Franz, M.; Larose, E.; Carrière, S.; Jongmans, D.; Jaboyedoff, M. Influence of environmental parameters on the seismic velocity changes in a clayey mudflow (Pont-Bourquin Landslide, Switzerland). *Eng. Geol.* **2018**, *245*, 248–257. [[CrossRef](#)]

64. Mreyen, A.S.; Micu, M.; Onaca, A.; Cerfontaine, P.; Havenith, H.B. Integrated geological- geophysical models of unstable slopes in seismic areas. In *Workshop on World Landslide Forum*; Springer: Cham, Switzerland, 2017; pp. 269–279.
65. Rezaei, S.; Shooshpasha, I.; Rezaei, H. Evaluation of landslides using ambient noise measurements (case study: Nargeschal landslide). *Int. J. Geotech. Eng.* **2018**, 1–11. [[CrossRef](#)]



© 2019 by the authors. Licensee MDPI, Basel, Switzerland. This article is an open access article distributed under the terms and conditions of the Creative Commons Attribution (CC BY) license (<http://creativecommons.org/licenses/by/4.0/>).